1967

An Experimental Ultrasonic Image System For Underwater Vision.

Robinson, Kenneth George.

Monterey, California. U.S. Naval Postgraduate School

AN EXPERIMENTAL ULTRA-SONIC IMAGE SYSTEM FOR UNDERWATER VISION

KENNETH GEORGE ROBINSON

AN EXPERIMENTAL ULTRASONIC IMAGE SYSTEM

FOR UNDERWATER VISION

by

Kenneth George Robinson
Lieutenant, United States Navy
B.S.E.E., University of Washington, 1958

Submitted in partial fulfillment of the
requirements for the degree of

MASTER OF SCIENCE IN ENGINEERING ELECTRONICS

from the

NAVAL POSTGRADUATE SCHOOL
June 1967

ABSTRACT

An experimental investigation of acoustic imaging in water is made at an ultrasonic frequency of 455 KHz. Using optical principles, the theory of image formation and resolution are discussed. The range capability of such a system is predicted by the use of underwater acoustic theory.

The apparatus consists of a basic imaging system that provides a set of d.c. voltages, proportional to sound intensity at points in the image plane, to be applied to a visual display system. Such a display will present a two dimensional image of an insonified underwater target.

This study differs from previous work done in underwater acoustic imaging, in that the image conversion process will lend itself to the application of integrated circuits.

TABLE OF CONTENTS

LIST OF ILLUSTRATIONS

TABLE OF SYMBOLS AND ABBREVIATIONS

B	bandwidth
c	velocity of sound in water
D	aperture diameter
f	frequency
F	focal length
F	noise figure
G	power gain
I	signal intensity
k	Boltzmann constant
λ	wave length
P	acoustic pressure in microbars
P	power in watts
r	range in meters
T	Kelvin temperature
T	target strength in db

ACKNOWLEDGEMENT

This project was suggested by Professor G. L. Sackman who acted as advisor. Sincere appreciation is expressed for his patience and many hours of helpful discussions.

Also, without the help of Mr. M.K. Andrews (head of the Physics Machine Shop), construction of the transducer image assembly would have been impossible.

1. Introduction

An effective acoustic imaging system providing real time visual information would be a significant adjunct to the detection and classification of underwater targets. Such a system would include collection of acoustic energy, signal conversion, and information display.

To date, no form of energy other than acoustic offers a promise of practical range capability and associated image resolution. In turbid water, vision by means of light is very limited, in some cases to a range on the order of one meter. With proper design, an acoustic imaging system of useable resolution should be able to "see" to a range of about 100 meters.

Previous work in the area of underwater acoustic imaging employed the use of an image converter Sokolov tube [4,8]. This was basically a cathode ray tube with a piezoelectric transducer plate in place of the glass face. The electrical charge distribution acoustically induced on the transducer modulates the scanning electron beam. It is this image converter tube that poses the basic limitation on acoustic imaging systems in which it is used. First, the mechanical construction of a sizeable piezoelectric face-plate sealed to the high vacuum tube make it inherently weak, vulnerable to the external pressure of atmosphere and being immersed in water. Secondly, the piezoelectric effect of the face allows no signal storage. Thus, the acoustic signal on the piezoelectric plate must be nearly a continuous wave to allow time for scanning. Furthermore, the energy arriving at a point not being scanned is lost.

Quartz and PZT plates have been used. However, lack of signal

storage coupled with the noisy electron scanning beam yield a relatively low converter sensitivity.

The purpose of this project was to investigate the practical aspects of acoustic conversion of the image with a signal storage ability. To accomplish this, a large number of identical amplifiers and detectors sense and store the acoustic signal for many sample points in the image plane. The investigation of the image sensor and subsequent signal processing comprise the basic acoustic imaging system. The resulting sensitivity is found to be considerably better than existing systems using the image converter tube. A reflective focusing system is applied in the form of a parabolic reflector.

2. Theoretical.

Due to their similarity in the fundamentals of wave propagation, the underwater acoustic imaging system is intuitively expected to closely resemble imaging systems utilizing light waves. The principle of the acoustic imaging system is then to form a focused image of a distant object that has been insonified by some means. Consequently, there can be associated with it an object plane, image plane, and a focusing system. While the basic fundamentals of light and acoustic wave propagation differ little, their specific parameter relationships differ greatly. Of these difference, the ratios of wave length to object detail and wave length to the aperture size are most pronounced. It is to be expected that the system parameters that relate to these specific relationships will differ quite widely.

The formation of information in the image plane by the focusing system is only the first half of the necessary function of a practical imaging system. The second half is the process of converting this acoustic image field in the medium to a form that can be easily interpreted by the human; the visual display. The method of producing a video display of the converted image field is treated in a thesis by LT. A.F. Barta [10].

Image Formation. A point object is assumed to scatter spherical waves. However, at long range (Fraunhofer region) the waves are approximately plane, allowing considerable mathematical simplification in analysis. More complicated wave front forms are assumed to be ensembles of plane waves. However, at short range this is not true, resulting in so called "near field" (Fresnel region) effects.

Figure 1 is a representation of a general reflective focusing

system. Two conditions must be met if plane waves arriving at A are to be focused at F. First, all of the wave energy arriving at F from plane A must be in phase. Second, the shape of the reflective surface O must be such that all of the captured wave front A is reflected toward F.

The first requirement means that all of the individual ray paths from wave front A to the point F via the reflective surface O must be of equal acoustic length. The second condition requires all rays to intersect at F. These two requirements specify the shape of the reflective boundary O. One surface satisfying the conditions, well known to the radar designer, is a parabolic reflector.

The resolution of such a reflective focusing system is easily determined utilizing optical fundamentals. The basic limitation in resolution is the inability to strictly satisfy the two conditions of the general reflective focusing system (aberration) and diffraction.

The image of a point source in the far field is described by Fraunhofer diffraction for a clear aperture to have an intensity of the form $\left(\frac{\sin x}{x}\right)^2$. Associated with this is the Rayleigh resolution limit $\Theta \approx 1.22 \frac{\lambda}{D}$ for a circular aperture [1]. A one dimensional depiction of the diffraction and resolution relationships is shown in Figure 2.

The determination of the best focal length for a given aperture of the reflective focusing system can be made by an analogy with photography principles. In photography there is nothing to be gained by making the optical system with greater resolution than the resolving power of the film. In Figure 2 then, the optimum ration for F/D will

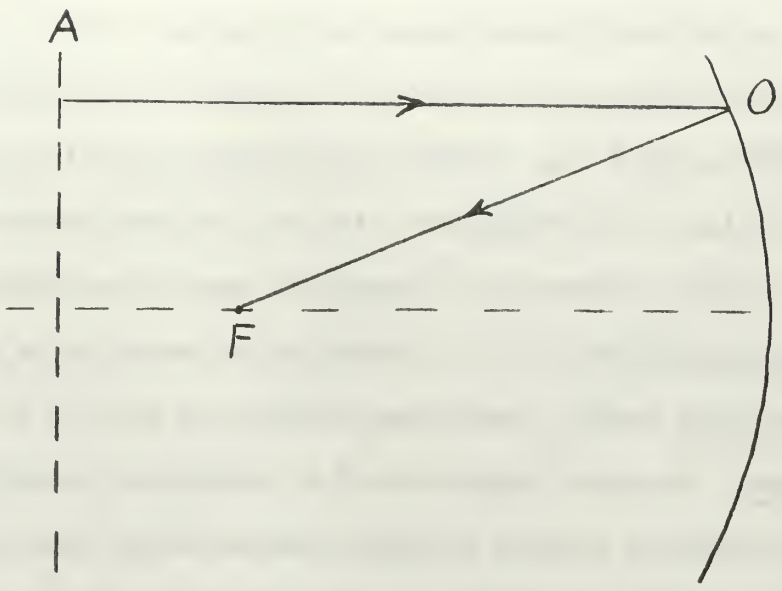

Figure 1. General Reflective Focusing System.

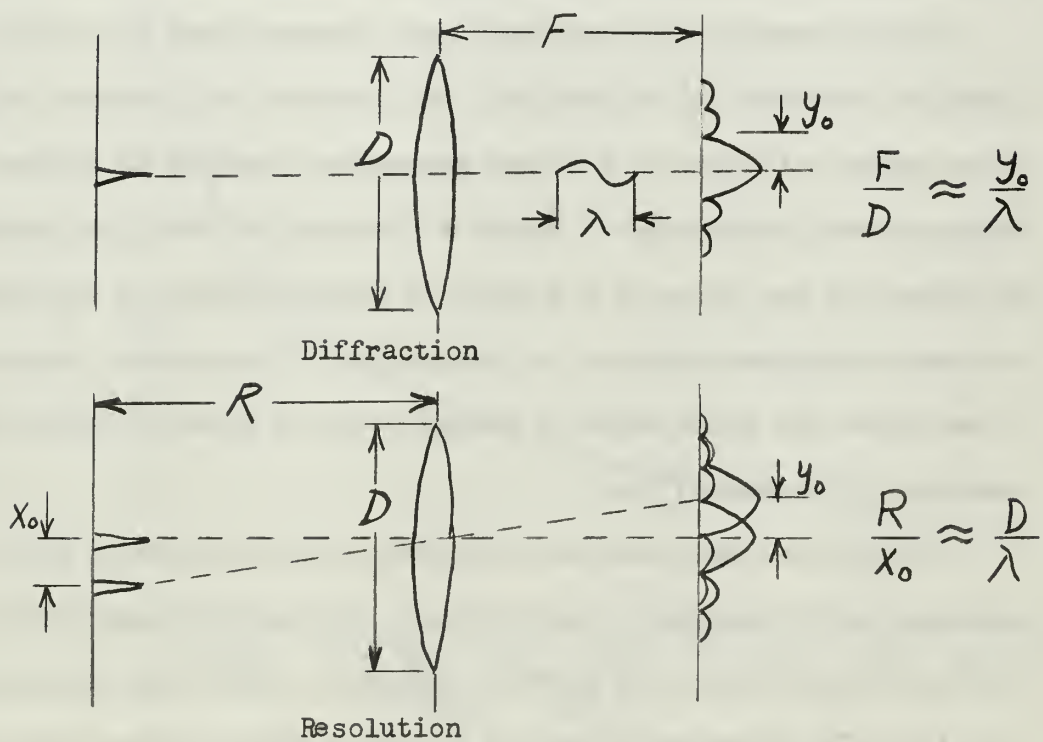

Figure 2. Diffraction and Resolution.

be determined by the resolution of the acoustic sensor in the image plane. An infinitely small sensor in an infinite baffle still has an effective area corresponding to a diameter approximately $\lambda/2$, equivalent to F/D $\doteq$ 1/4. However, practical constraints on the transducer limit the transducer size to a minimum diameter near one wave length. Furthermore, geometric aberrations degrade the off-axis focusing ability of a parabolic reflector at values of F/D less than about unity. Therefore, ratios near F/D = 1 are near optimum.

Range. The range capability of an underwater acoustic imaging system is severely limited by sound attenuation at high frequencies. There is attenuation in the medium due to viscous absorption. This loss is proportional to the square of the frequency, and the required frequency region that will allow one to approach a realizable image forming system makes it a serious concern.

Total attenuation is dependent upon frequency and also upon the molecular structure of the medium. The presence of dissolved salts in sea water will give it a higher absorption constant at a given frequency than fresh water. Beyond a frequency of about one megahertz the effect of the salts in sea water is negligible and it approaches the same absorptive constant as fresh water. The acoustic absorption of sea water and fresh water in db per meter is shown in Figure 3 as a function of frequency [2].

In addition, spherical acoustic waves suffer intensity loss inversely as the square of the distance. The spherical spreading loss for two way travel is shown in Figure 4. This loss is proportional to r^{-4}, expressed by 40Xlog (r) for a diffuse target since the spherical center of reflected waves is assumed to be at the target.

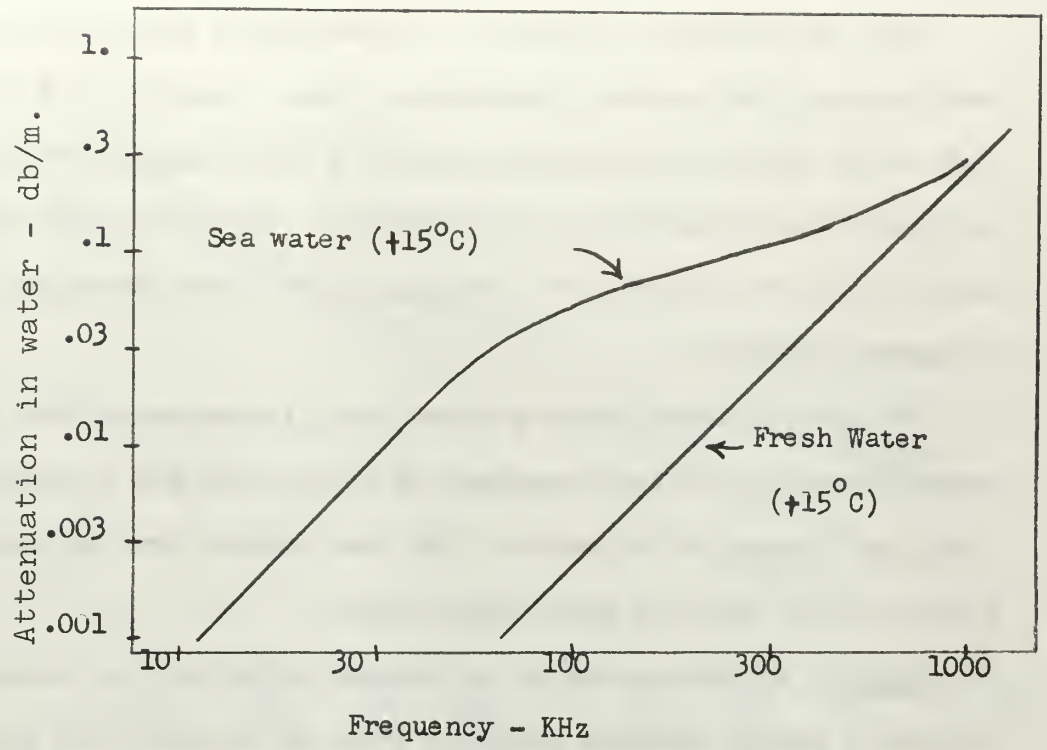

Figure 3. Ultrasonic Absorption in Water.

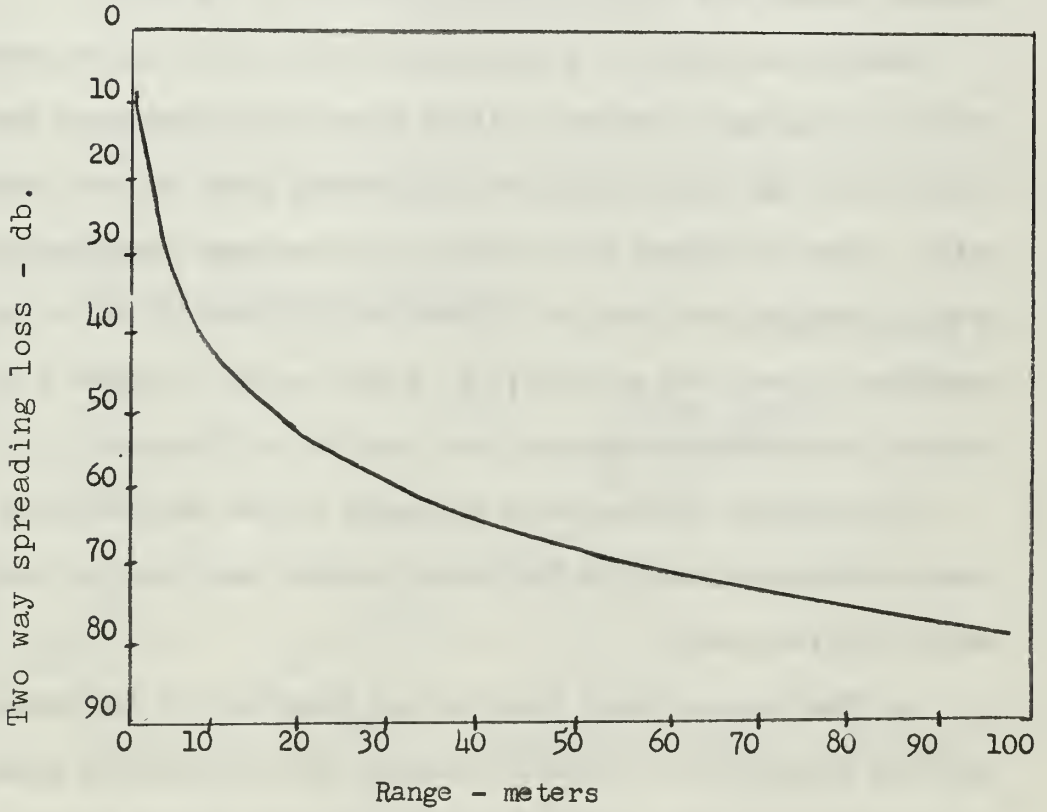

Figure 4. Two Way Spherical Divergence Loss.

When the effects of spreading and absorption losses are combined, they comprise the acoustic transmission loss. Figure 5 is a composite plot of the two way transmission loss at a water temperature of 15° centigrade for three different frequencies. Fresh water has been assumed as it will have direct meaning in the later laboratory experimental results.

The effect of frequency upon the total transmission loss is remarkably shown in the comparison of loss at 100 KHz to loss at 1 MHz, at a range of 100 meters. The loss changes from approximately 80db to 120db, which is quite significant.

Noise. Ambient sea noise and thermal noise are the basic sources of electro-acoustic converter noise in an underwater acoustic imaging system.

Ambient sea noise is a resultant of all of the noises generated within the medium of the sea. It is generally acknowledged that the surface wind and wave action are the primary cause of this ambient noise. Shown in Figure 6 is a plot of the average pressure spectrum level of ambient sea noise as a function of frequency for a sea state condition of zero and no wind [2]. Also plotted in Figure 6 is the thermal noise spectral density as a function of frequency.

In comparing the two plots of Figure 6, the thermal noise becomes predominant above 50 KHz, while ambient sea noise is predominant below this frequency.

In "The Thermal-Noise Limit in the Detection of Underwater Acoustic Signals", R.H. Mellen discusses the relationship between the parameters of the receiving system and the ambient noise level of the medium [3]. He arrives at an expression that relates the

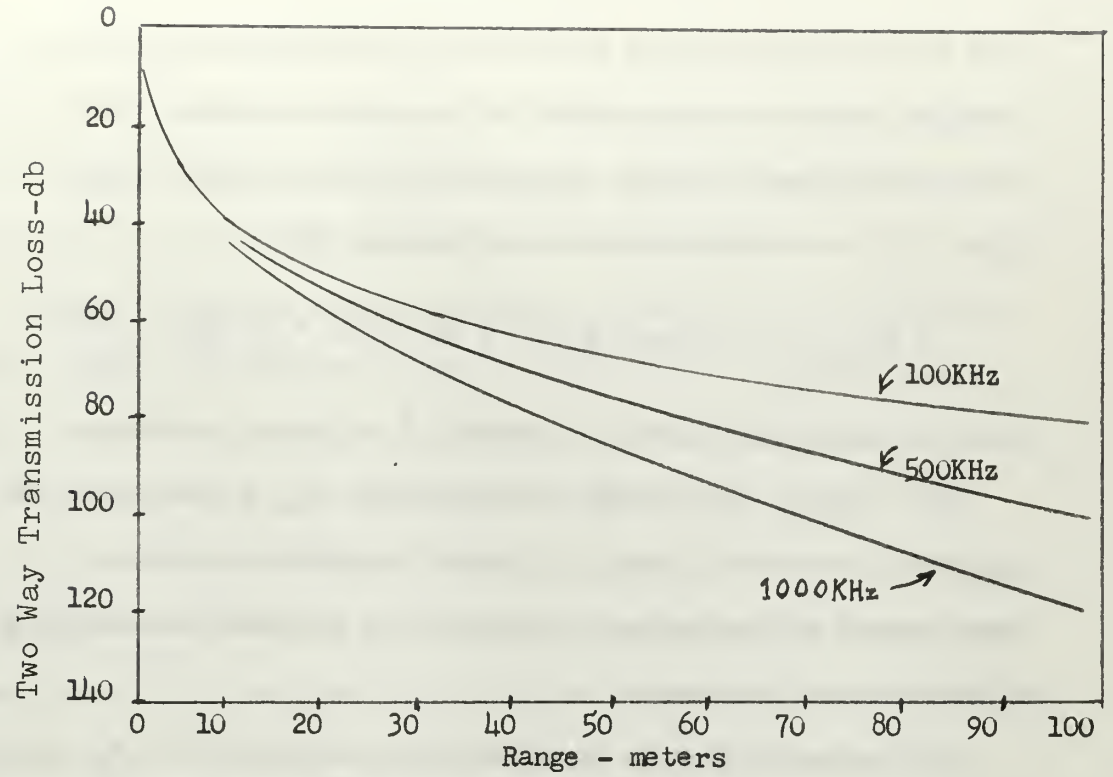

Figure 5. Two Way Transmission Loss

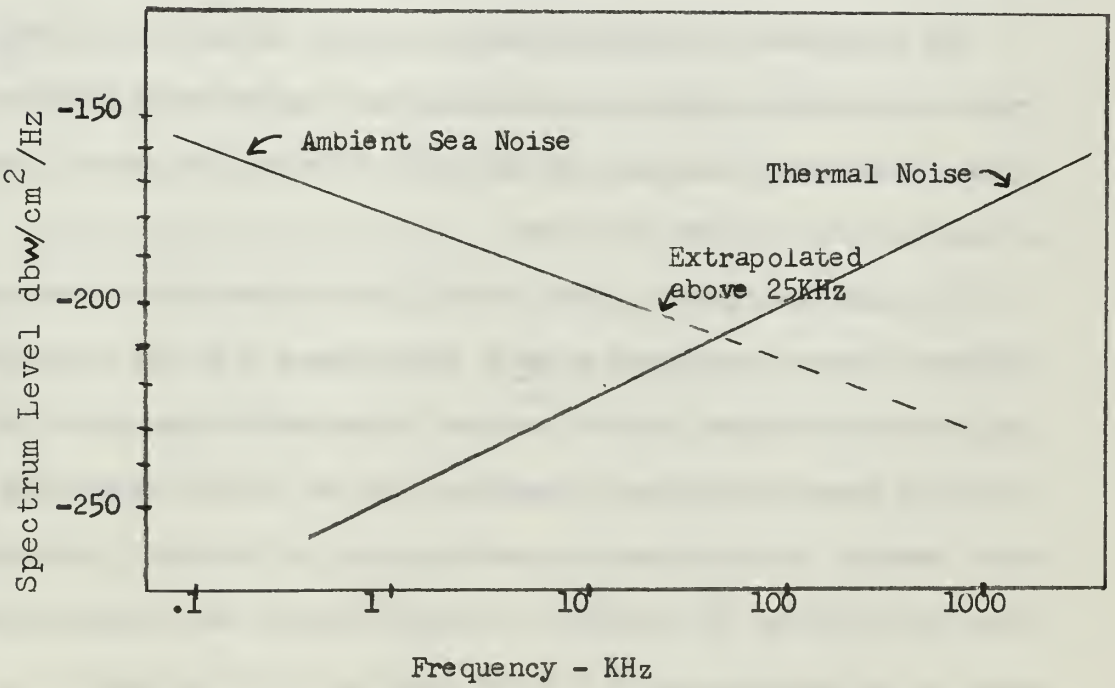

Figure 6. Thermal and Sea Noise Spectral Density

plane wave acoustic signal intensity (I_s) required for unity electrical signal-to-noise ratio to the system parameters of directivity ($D\theta,\phi$), ambient temperature (T), amplifier noise figure (F), and electro-acoustic efficiency (η):

$$I_{S(S/N=1)} = D(\theta,\phi)\frac{4\pi f^2}{c^2} k\, Ta\, \Delta f\left[1 + \frac{T}{Ta}\left(\frac{F}{\eta} - 1\right)\right]$$

where c = velocity of sound in water, k = Boltzmans constant.

This assumes that $f \gg \Delta f$ and that $D(\theta,\phi)$, T_a, F, and η can be considered constants. Here, T_a is the equivalent acoustic "temperature" of the medium, obtained from the ambient noise level at the operating frequency.

The bracketed term is important only when the ratio $\frac{T_a}{T}$ is small compared with the ration F/η. For example, at 10 kHz $T_a/T \approx 100$ for sea state zero. The ratio F/η need only be of the order of 100 to be within 3db of a perfect hydrophone and amplifier.

The importance of this expression becomes apparent at higher frequencies as the ambient sea noise becomes dominated by thermal noise. Here, the efficiency of the hydrophone and the noise figure of the amplifier become important.

In general the noise power density in the transducer's radiation resistance can be expressed as $\frac{Pn}{A} = kTB/A$, where A is the effective area of the transducer that is coupled to the medium and B is the effective bandwidth of the transducer. At the higher frequencies where thermal noise becomes appreciable, the efficiency of the transducer only affects the transfer of signal energy, but allows thermal noise to be present without being reduced by the efficiency.

The result of this noise analysis, is to emphasize the importance of transducer efficienty in conjunction with noise figure and its effect upon system sensitivity at the high frequencies required for a practical acoustic imaging system.

Target Strength. The next acoustic parameter to be considered in the medium is the target itself. The acoustic energy reflected from a target is a function of the impedance mismatch between the target and the water, and the size and shape of the target.

The ratio of reflected to incident intensity is $\frac{I_r}{I_s} = \left| \frac{\rho c - \rho_o c_o}{\rho c + \rho_o c_o} \right|^2$ where ρc is the acoustic impedance of the target and $\rho_o c_o$ is the acoustic impedance of the water [2]. The value of this reflection ratio for typical solid metals in water ranges from about 0.5 to 0.9.

The directivity function that includes the size and shape of the target along with the reflectivity can be shown to be $T = 10x \log \frac{\sigma}{4\pi}$ where σ is the effective scattering cross-section of the target [2]. This target strength is derived from a reference strength of 0db for a perfectly reflecting 2 meter diameter sphere.

Scattering and Reverberation. Any body of water that is exposed to a natural environment has within its medium a large number of internal acoustic scatterers. These may vary from small thermal discontinuities to air bubbles and to sizeable objects such as fish. The combined effect of scattered acoustic energy from these irregularities back to the transmitter-receiver system is called reverberation, and as such may lead to the masking of the desired signal return.

The two parameters involved with these scatterers are their

effective cross-section σ, and total number n per unit volume. [illegible] the assumption that the volume scatterers reradiate omidirectionally, it can be shown that the resultant reverberant acoustic return as a function of range r is equivalent target strength of

$$T_R = 10 \times \log \frac{n\sigma r^2 \Delta r \Omega}{4\pi} \qquad [2]$$

where Ω = solid angle of enclosed volume, or

$$T_R = 10 \times \log n\sigma + 20 \times \log r + 10 \times \log \frac{c\Delta t}{2} - dr$$

where dr = directivity ratio.

The term 10 x log ($c\Delta t/2$) is indicative of the improvement obtained in overcoming backscatter masking by the use of pulse operation. The reverberation will not become significant until it equals or is greater than the actual acoustic strength of the target of interest.

Typical values of $n\sigma$ range from 10^{-6} to 10^{-7} meters^{-1}. For a 0.2 millisecond pulse duration, $\frac{c\Delta t}{2}$ = 0.15 meters. Assuming the receiver has a directivity ratio of about 30db and the maximum range is 100 meters, $T_R \simeq -60 + 40 - 8 - 30 = -58$ db.

An attempt to estimate the composite effect of the system parameters described is given below.

Assumptions

Frequency	455 KHz
Receiver aperture	1 meter
Receiver bandwidth	5 KHz
Amplifier noise figure	10 db
Target strength	-10 db
Range	100 meters

Noise Estimate

Thermal noise	-185 db/Hz
Aperture directivity	-30 db
Noise bandwidth	37 db
Noise figure	10 db
Net noise	-168 db

Signal loss estimate

Spherical divergence	80 db
Viscous attenuation	20 db
Target strength	10 db
Net Loss	110 db

Assuming a unity signal-to-noise ratio; 110-168 = -58db source strength is required. This corresponds to about 10^{-6} w/cm^2 at one meter radius from the transmitter which is quite attainable without being overcome by cavitation. The above system analysis does not include the F/η effect on noise. If the transducer efficiency η, becomes less than the noise figure F of the amplifier, then the effective noise figure for the system approaches $1/\eta$.

3. Design Considerations.

Starting with the premise that the resolution will be the important characteristic of an underwater acoustic imaging system and that the system must be physically reasonable in size, the following can be proposed:

a) $D/\lambda > 100$.

b) $D \sim 1$ meter.

c) Resolving distance in image plane $\sim\lambda$, will yield an $F/D \sim 1$.

d) A wavelength λ of 1/100 meter or less.

e) Assuming velocity of sound in water to be 1500 m/s, the frequency will be $>$ 150 kHz.

With a lower bound on the frequency desired for the system, a consideration was made involving available amplifiers in this region. A miniature transistorized I.F. amplifier tuned at 455 kHz was available through the Miller Company (type 8902-B) at a reasonable cost. This frequency placed the wave length in water in the order of 3 millimeters.

Several segmented PZT-5 (Lead Zirconate Titanate) piezoelectric transducer arrays cut to 455 kHz resonance were obtained from the Mine Defense Laboratory, Panama City, Florida. Figure 7 depicts the mechanical construction of the transducer array shown along side one I.F. strip.

In the completed prototype system, the size of the array is 9X9 or 81 elements. Every other element in the segmented array is an active one, with the rest left unconnected electrically. The dimension of each element is 1.5x1.5 millimeter. This results

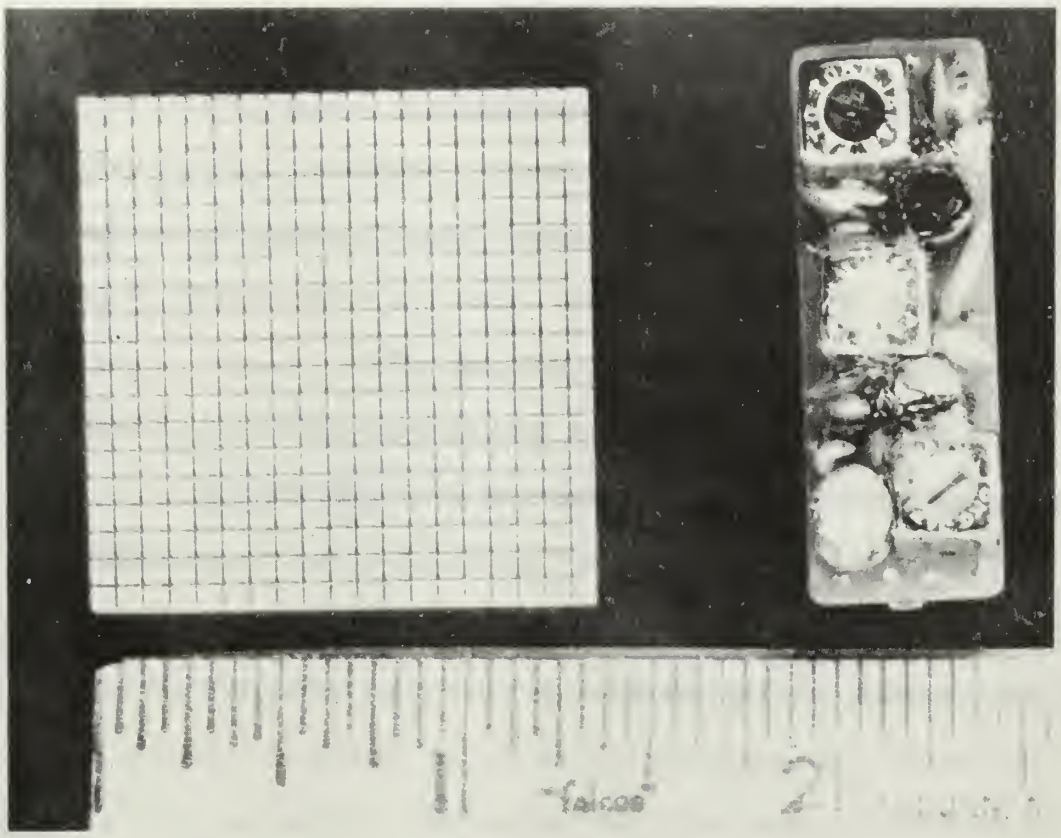

Figure 1. I.F. strip and transducer array

in the image sensor having approximately one wavelength resolution.

Assuming each element to be representative of a longitudinal half wave vibrator, two transducer parameters were theoretically predicted. The water loaded output impedance of an element was calculated to be about 3.5 k ohms, while the electro-acoustic response E/P was calculated at approximately $1.5X10^{-6}$ volts/microbar.

An aluminum parabolic reflector was acquired in accordance with the estimated parameters. The actual figures pertaining to the reflector were D = 79cm, F = 55cm. Thus $D/\lambda = 242$ and $F/D = 0.7$. The surface accuracy was on the order of $.25\lambda$.

The theoretical gain for the aperture can be computed from the expression $G = 4\pi A/\lambda^2$, resulting in G = 57 db [5].

With these basic components the next step was to consider the design problems and perform experimental tests on the various parts of the acoustic imaging system.

4. Experimental.

The initial test was that of obtaining a basic diffraction pattern of a point source. To accomplish this, a single array transducer element was traversed across the front of the aperture in the focal plane. The results of the experimental test yielded the basic resolution of the imaging system. In addition, it provided a qualitative indication of aperture phase error due to manufacturing tolerances in spinning the aluminum parabolic reflector.

Figure 8 shows the anechoic tank arrangement for the test. A pulse width of 0.25 milliseconds was used in order to separate the surface reflections that were apparently scattered from the aperature edges.

In addition to the pulsed coherent wave pattern, a diffraction pattern for frequency modulated acoustic pulses was investigated. Figure 9 shows the result of the pulsed coherent wave diffraction pattern. No appreciable difference was noted when a 1% frequency modulation was applied to the pulse.

The semi angle to the first null is .26°. This compared well with the theoretical value of $\theta \cong 1.22\lambda/D$ or .25°. The first side lobe level is about -10db below the main lobe. The theoretical value for a uniformly illuminated circular aperture is -17.6db [5]. The definite side lobe raising here was caused by phase errors in the reflector and aperture blocking by the transducer array.

During this same experimental phase the aperture gain was measured. This was accomplished by removing the reflector and turning the transducer array around to measure the incident acoustic energy

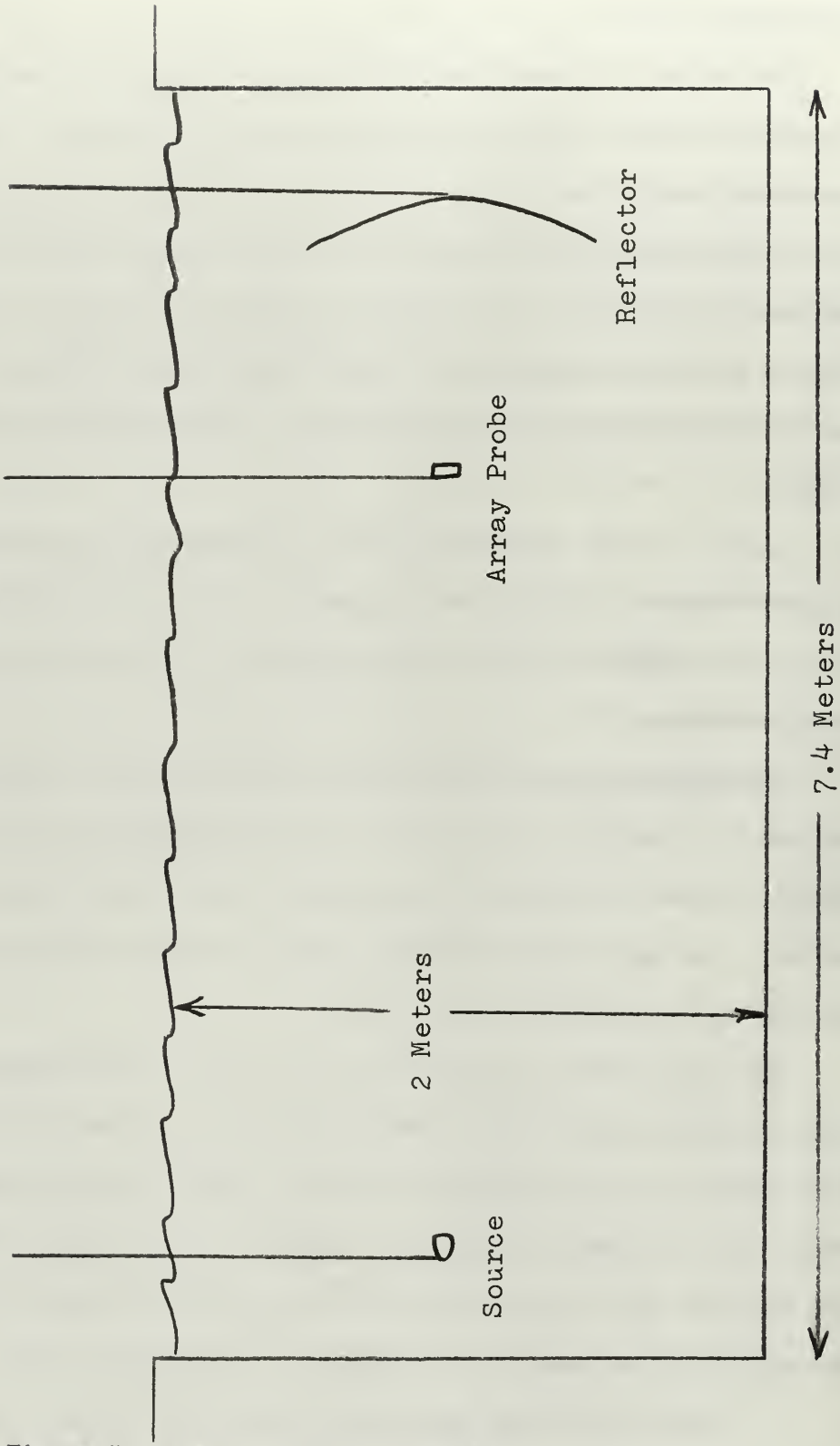

Figure 8. Anechoic Tank Probe Test

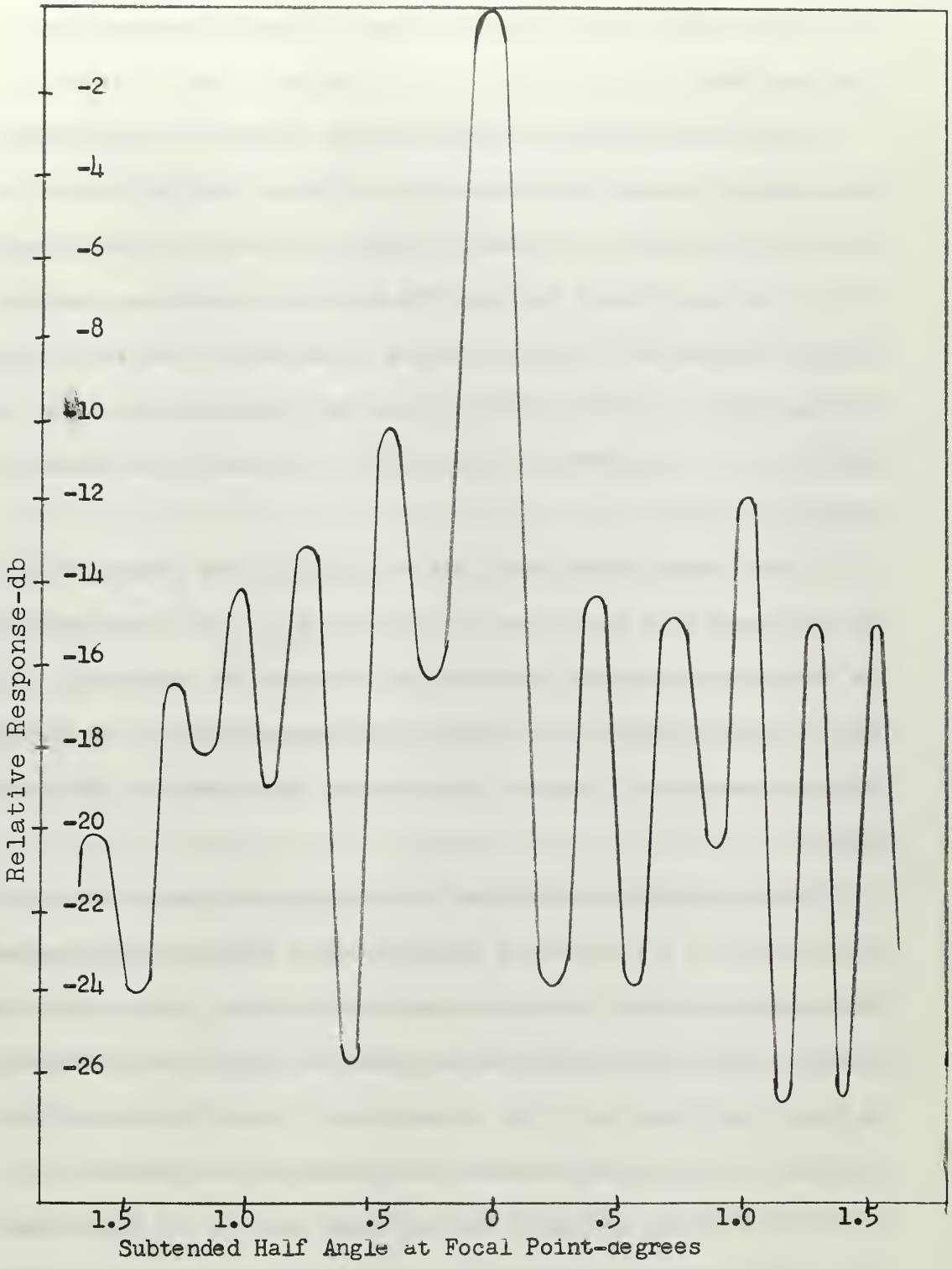

Figure 9. Aperture Response for Pulsed Coherent Waves

and comparing it to the focused energy. The resultant aperture gain was 18db.

A major discrepancy appeared when the measured aperture gain was compared to the theoretical gain of 57db. This difference occured due primarily to the short range, the object distance being well within the Fresnel region. The theoretical gain was computed using an expression valid only in the Fraunhofer or far field region. The approximate boundary between these two regions occurs at an axial distance from the aperture of about $D^2/2\lambda$ or 96 meters for this system [5].

A near field directivity gain reduction on the order of 35db was estimated from the curves of reference [6]. The aperture blockage and phase errors are accountable for about 7db reduction. Applying this total reduction of 42db to the theoretical gain of 57db, the resultant net gain is 15db. This compares quite well to the measured 18db.

The sensitivity calibration of the image transducer array was accomplished by a reciprocity method using a USRD type E8 transducer. The voltage response to incident acoustic pressure on the individual elements of the array (E/P) was measured as $4.7X10^{-6}$ volts/microbar. As this measurement was being accomplished, it was noted that the combined effect of the transducer and the amplifier produced a 4 millivolt peak-to-peak noise level. Using this as the lower limit for minimum detectable signal, the sensitivity of the image array is -111dbw/cm^2. This figure compares very favorably with the sensitivity figure of -70dbw/cm^2 obtained in earlier work done with the Sokolov tube [4].

The theoretical absolute minimum detectable signal can be derived in a simple fashion. For a simple source in an infinite baffle, the directivity gain is 2 [2]. Using this and the gain relation $G=\frac{4\pi Ae}{\lambda^2}$, the effective capture area for one transducer element can be calculated. The thermal noise power density Pn/Ae is then calculated from kTB/Ae. The parameters for the system yield a thermal noise limit of $1.23X10^{-15}w/cm^2$ ($-114dbw/cm^2$).

The measured sensitivity of $-111dbw/cm^2$ infers a threshold of 30db over thermal moise. Previously, an estimate of about $10^{-6}w/cm^2$ source strength was predicted for a range of 100 meters. If the 30db threshold value is applied a more realistic value of $10^{-3}w/cm^2$ is required.

Using nine elements in one row of the array, a measure of mutual effect or cross-talk between elements was made by a reciprocity method. By electrically exciting the first element in the row, the response of the successive eight elements was measured. Figure 10 shows the array element cross-talk for a 40mv peak-to-peak signal applied to the first element.

Considerable time was spent in the testing and redesigning of the Miller 8902-B I.F. strips before they were acceptable as channel amplifiers.

It was determined that the desired signal processing method within this part of the imaging system would be simply a peak pulse detector. As shown in the circuit diagram of Figure 11, the amplifier consisting of an I.F. strip includes a built in detector. However, the output of the amplifiers had to be modified in order that the channel time multiplexing system be able to read the output

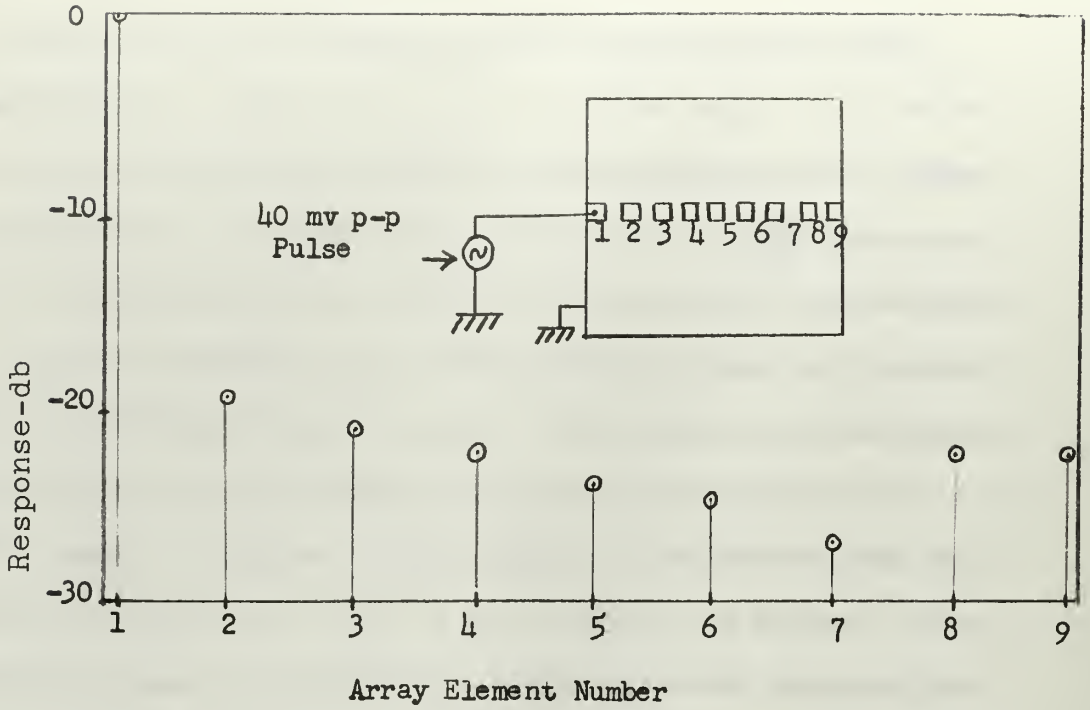

Figure 10. Acoustic Cross-Talk in Transducer

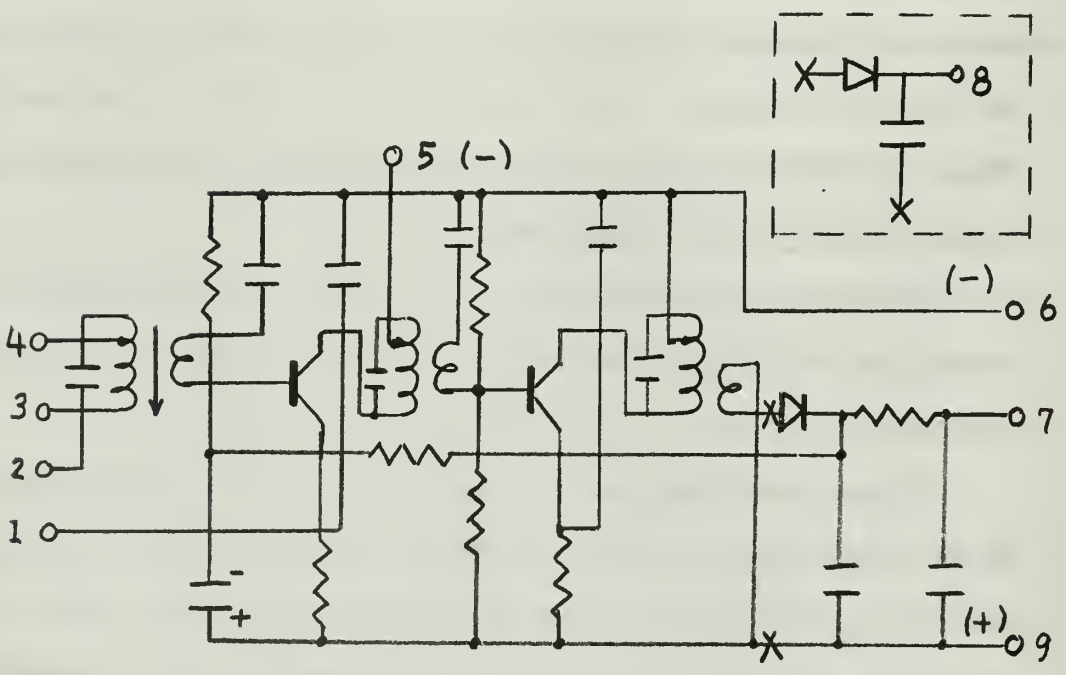

Figure 11. Circuit Diagram of I.F. Strip

of each channel before the stored signal decayed. The detector was originally designed for broadcast A.M. demodulation, and its time constant was not large enough to hold a signal for the approximate pulse repetition rate of 10 milliseconds. Here, a redesigned detector was put in place of the original, comprised of a 1N276 diode and a 0.1 microfarad storage capacitor.

The removal of the original envelope detector also dissabled the AVC network. With those changes made, the measurement of the amplifier's output vs. input characteristic was made. Figure 12 is the resultant curve using inputs 4 and 2 with-8 volts collector supply.

Consideration was then given to the problem of range-gating the channel amplifiers. An effective gate design would entail 81 separate input gates. The component quantity required for such a design appeared formidable in addition to the already multiplying number of channel components. With this in mind, the use of a pulsed power supply to the amplifiers seemed to be the answer, since it would be simultaneously applied to all amplifiers.

In testing a pulsed power supply scheme, it was found that the transformer coupled stages of the amplifier produced large switching transients concurrent with the turn off time. Since this transient spike was larger than any expected signal, the peak reading diode held the spike level leaving the signal undetected.

Series insertion of a 200 mh inductor reshaped the power supply pulse such that the switching transients disappeared compared to any expected signal level. This solution introduced an additional problem. The time constant required by the reshaped pulse power

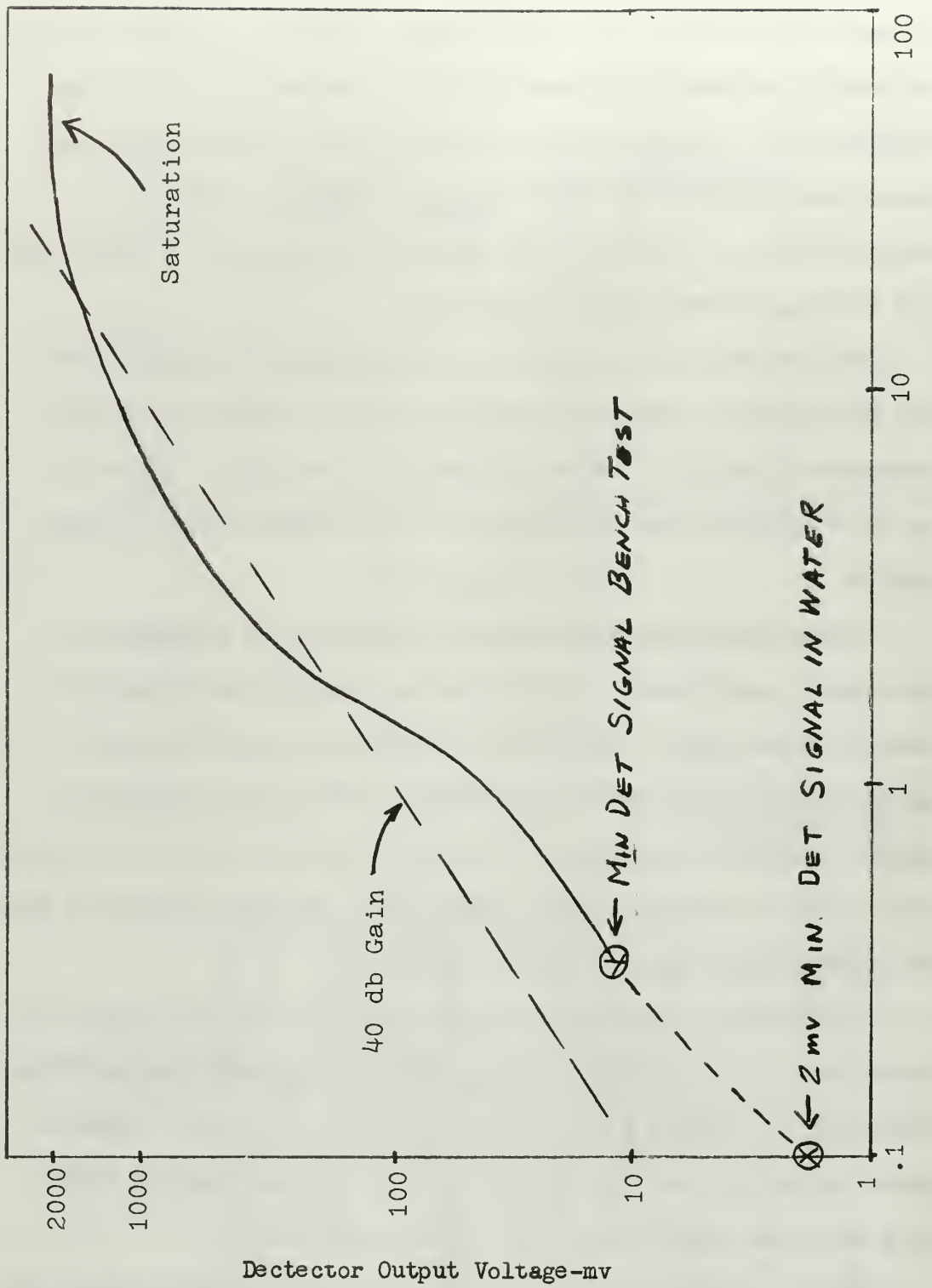

Figure 12. Output vs Input of I.F. Strip

supply absorbed approximately 80 percent of the designed 10 millisecond pulse repetition rate. This made a very ineffective range gating system. At this point it was decided to revert to a simple D.C. supply. In addition, the controlled conditions of the experiments applied to the imaging system in the anechoic tank did not make the use of an effective range-gate immediately important. Figure 13 shows the pulse output waveform before detection. Figure 14 is the detector output waveform.

An assessment of channel cross-talk was made for the other stages of the system. Previously mentioned was the mutual effect of the transducer elements. Figure 15 shows 18 channel amplifiers mounted on a $4\frac{1}{2}$" x $5\frac{1}{2}$" Vector board. With the amplifiers in the final closely packed mountings, the cross-talk between them was no worse than -40db.

The last area of cross-talk considered was the 82 conductor cable used to connect the image array to the above water electronics. The cable used was a Belden 8283 T.V. Color Camera Cable. Within the cable, sets of 5 unshielded wire were twisted together. Among these 5 wires the cross-talk was found to be about -15db, with no appreciable cross-talk among adjacent sets of these 5 twisted wires.

A block diagram showing the underwater acoustic imaging system with the video signal to the display unit as the output is shown in Figure 16.

Figure 17 depicts the construction of the 81 channel (9X9 array) image transducer assembly. It is mounted at the focal point of the reflector and has a mechanical focusing drive attached.

Since the focal point of the reflector is well within the Fresnel

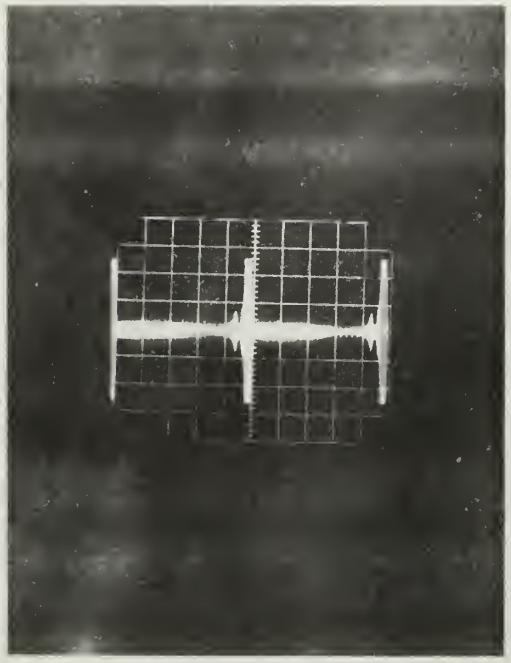

V-Scale:
200 mv/cm
H-Scale:
2μs/cm

(Time axis reversed)

Figure 15. Pulse output of L.F. strip

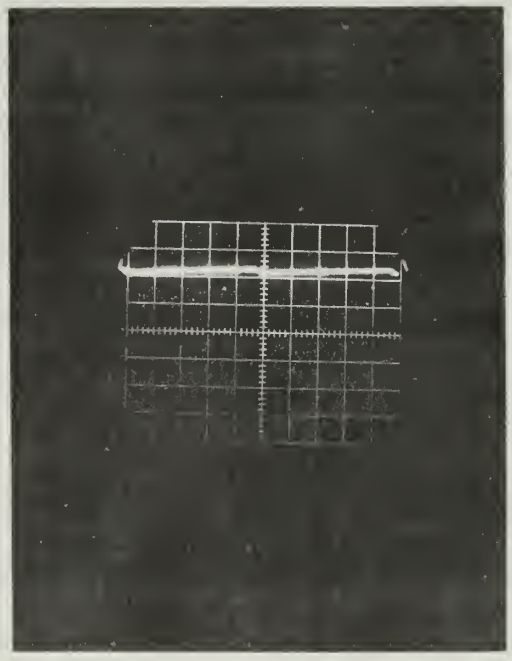

V-Scale:
200 mv/cm
H-Scale:
2μs/cm

(Time axis reversed)

Figure 16. Detector output

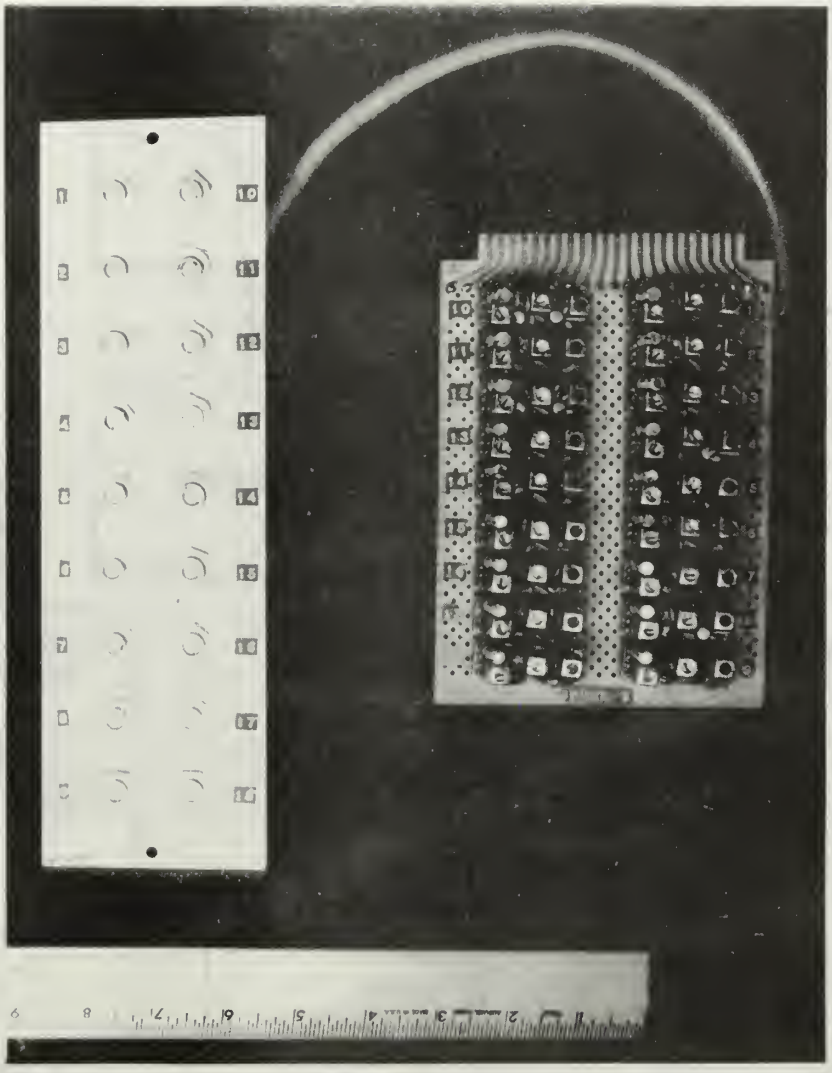

Figure 15. Mount [illegible] ters

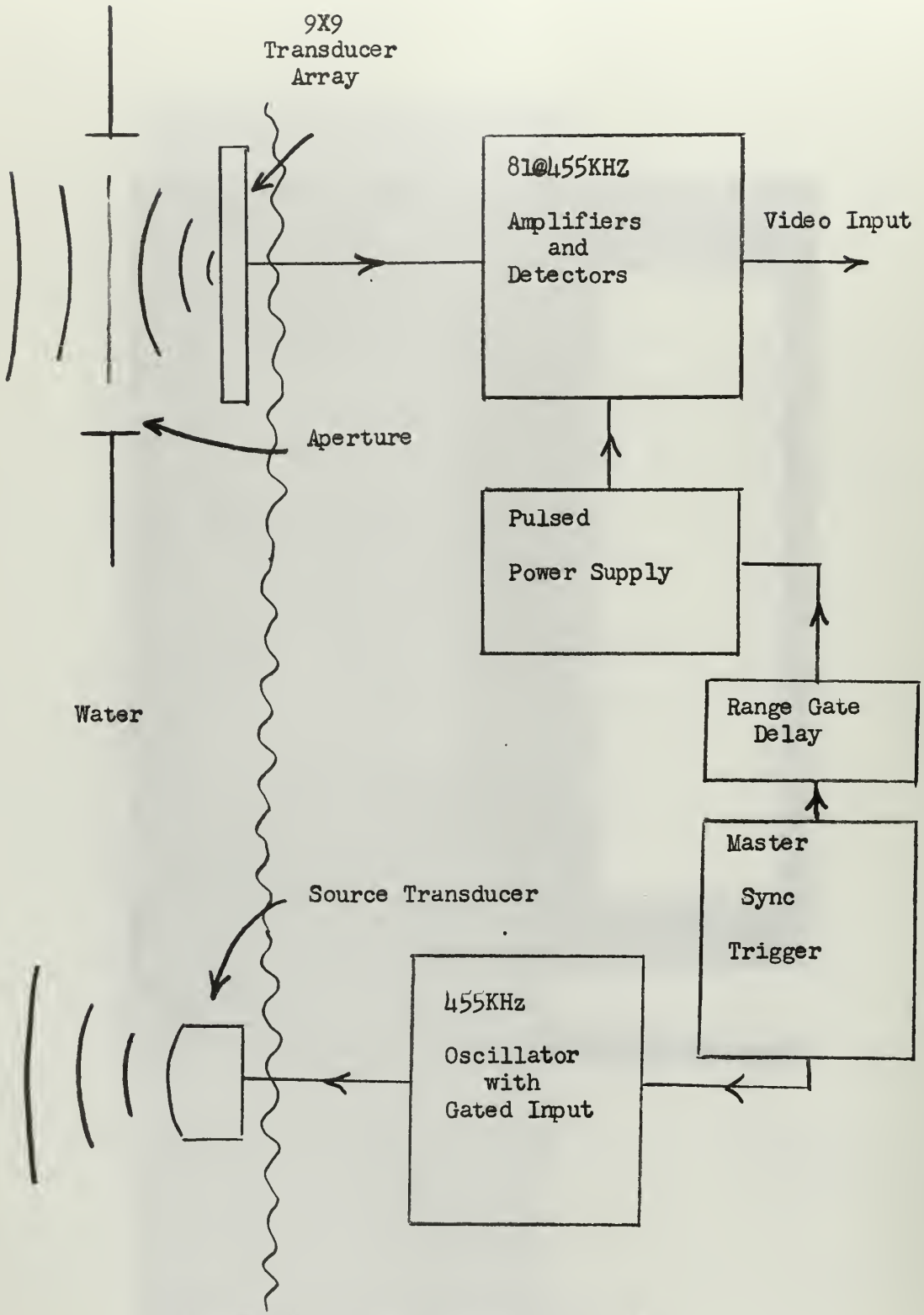

Figure 16. Block Diagram of System

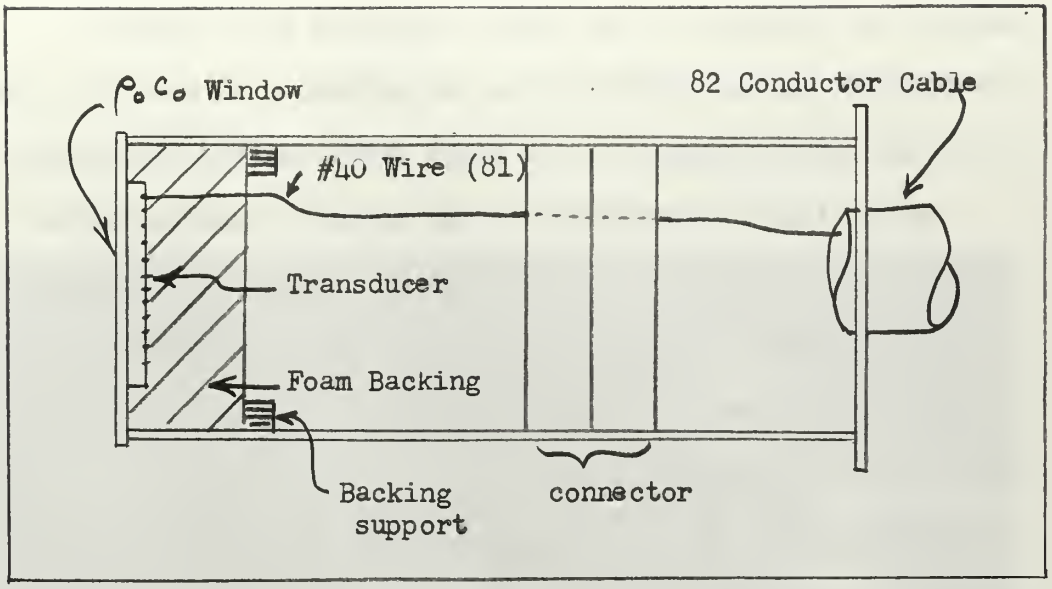

Figure 17. Acoustic Imaging Transducer Assembly

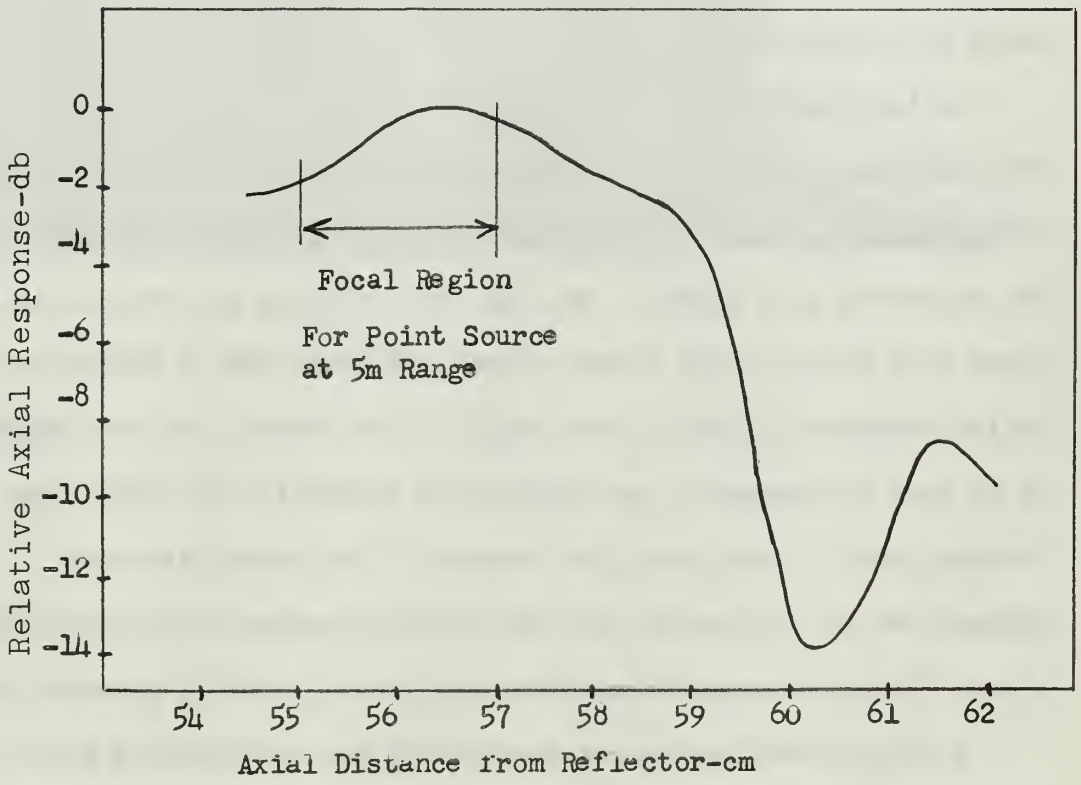

Figure 18. Axial Focusing Response

region, the response of the image transducer will undergo fluctuations as the distance from the reflector is varied. Figure 18 is the axial response of the image array to focusing action.

At the time of completion of the acoustic imaging system (shown in Figure 19) the channel time-multiplexing system and video display were not completed. As a result, all 81 channel output voltages had to be measured manually. This limited the final testing procedure severely.

A test image was formed using a small 2cm diameter transducer as a point source at a range of 5.5 meters. The 81 element array as designed has a field of view of $\pm 2^{o}$. This corresponds to a 38.5 cm field dimension at 5.5 meters. Figure 20 is a graphical reconstruction of the intensity response of the image array to the point source.

An investigation of the system resolution was made using two transducer point sources separated laterally by 18cm at a range of 4.9 meters. Figure 21 shows the image produced by this test. The separated main lobes of the two point sources are visible in the lower half of the image array. Since the array has an effective field dimension of 34cm at the range of 4.9 meters, the two images do in fact correspond to an approximate separation of 18cm. The "bright spot" in the upper left corner of the image plane was perhaps due to scattering from the reflector-array support structure. A more effective acoustic aperture stop would probably prevent this.

A final investigation on sensitivity was accomplished with a reflective target. The target was a 2cm diameter air filled sphere positioned at a range of 5 meters. The following conditions were

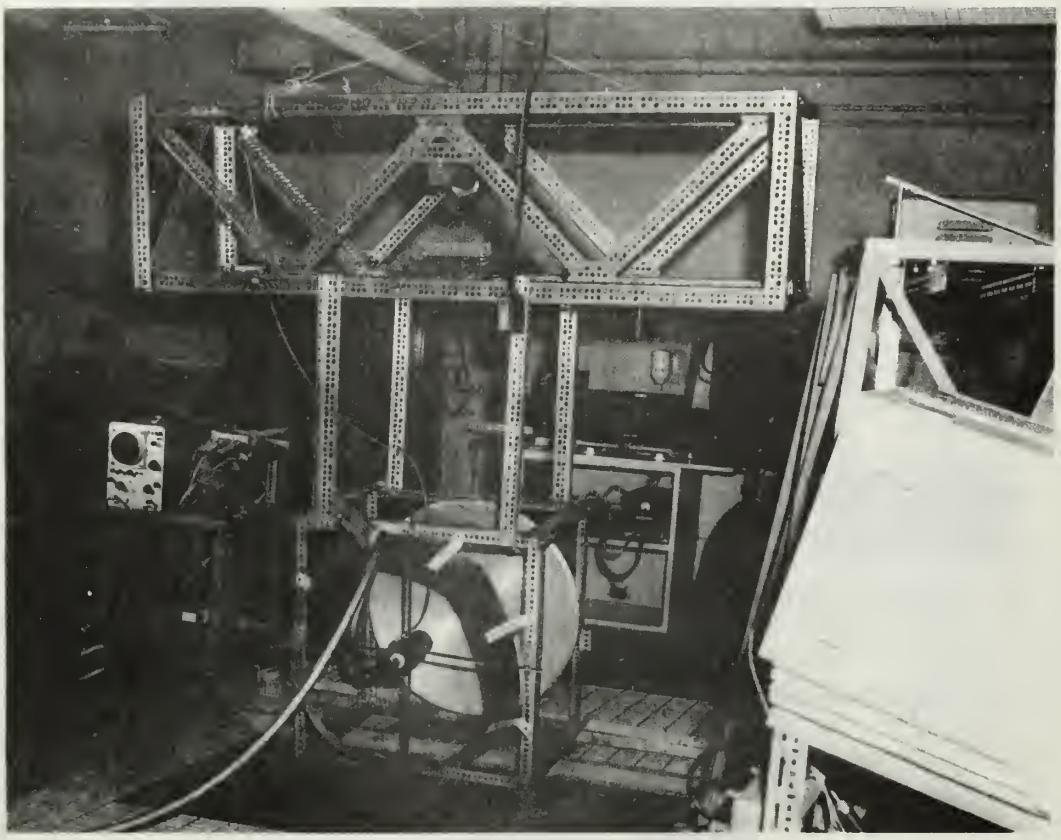

Figure 19. Acoustic Imaging System

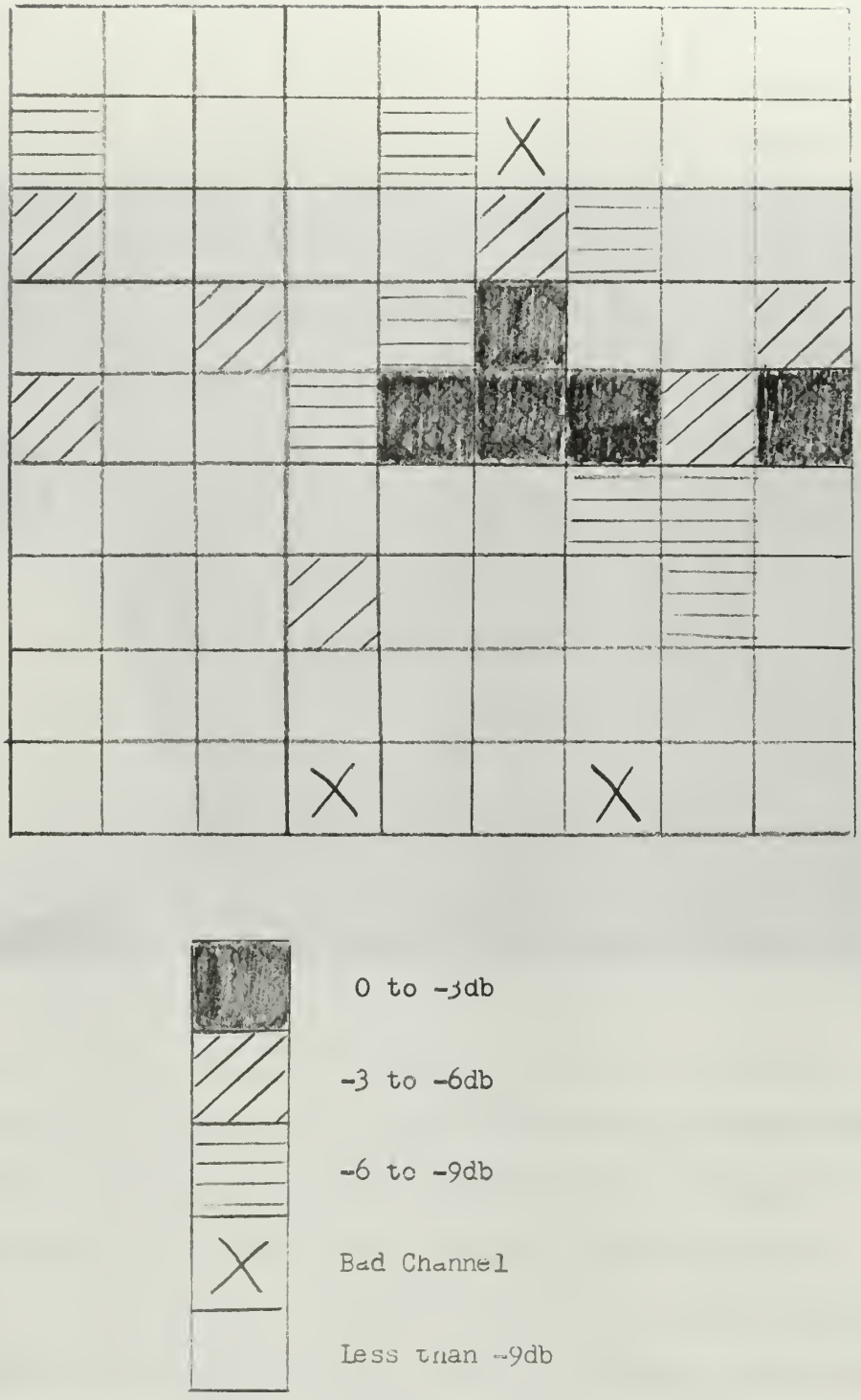

Figure 20. Intensity Response of Image Array to Point Source

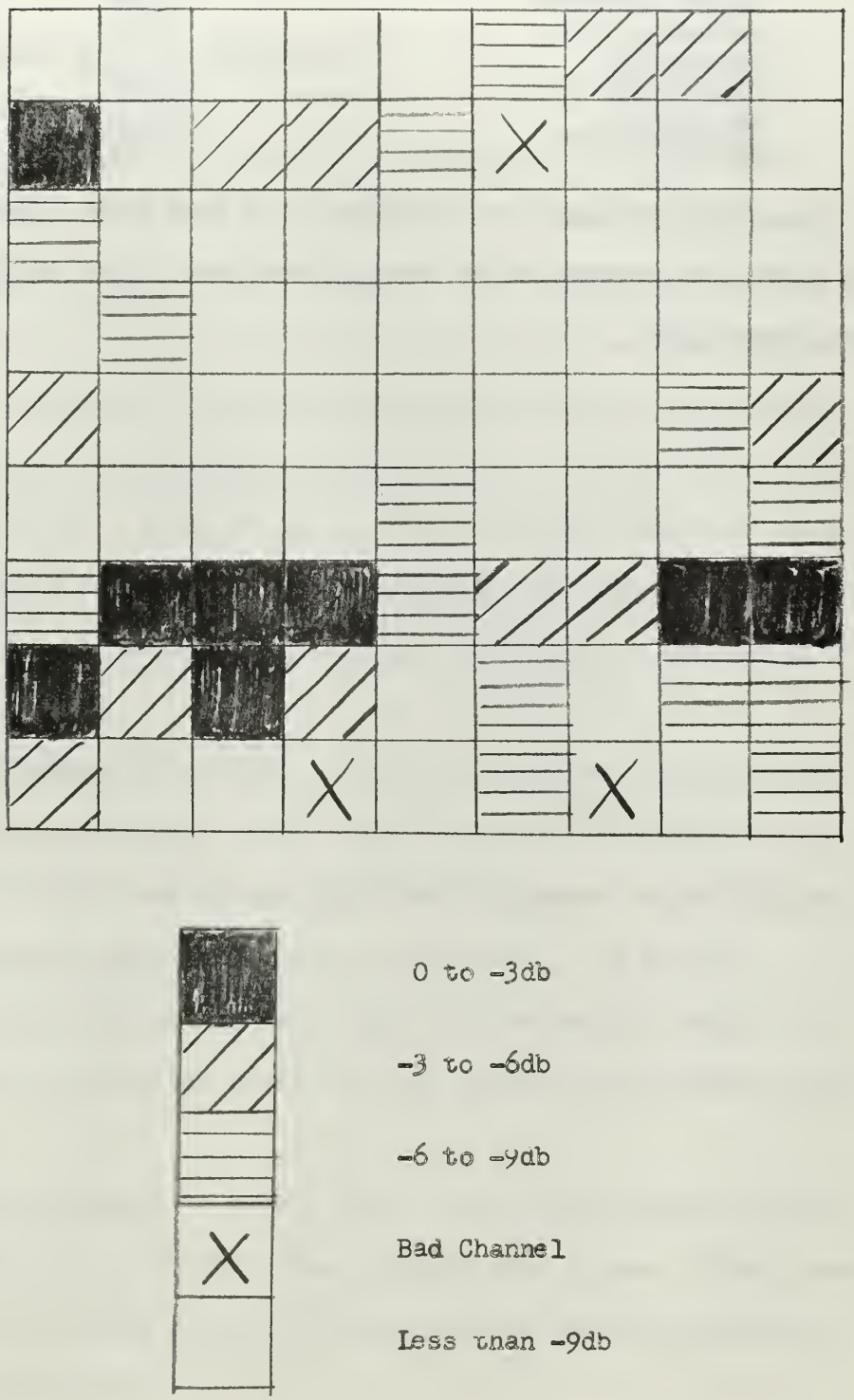

Figure 21. Intensity Response of Image Array to Two Point Sources

applicable to the experimental test.

Acoustic power	-20db
Target strength	-40db
Spreading loss	-28db
Absorption	(negligible at this range)
Net signal	-88db
Sensitivity	-111db
Net S/N	23db

The output voltage for this target was 40mv peak. This is 26db above the observed noise level of 2mv peak. Thus the results agree within 3db.

5. Conclusion.

The present system could be improved by apperture shading. With proper absorbtive acoustic tapering of the reflector (such as Gaussian) the suppression of side lobes could be effected, thus reducing the confusion caused by the diffraction ring pattern.

The field of view of the experimental system is very limited. Any extensive increase in the field (a 30X30 would seem necessary for effective imaging) would produce detrimental aperture blockage. The next natural step in designing an operational acoustic imaging system would be the investigation and use of a liquid filled lens. This would allow a large field of view without the aperture blockage associated with the reflective system. The liquid lens would allow some means of shading with proper selection of indices of refraction.

The fundamental results of this investigation indicate that an effective image array sensor that is directly connected to the associated channel amplifiers and storage elements can be designed to have a sensitivity of at least -111dbw/cm^2. The 455 KHz frequency of operation has been shown to give useable range with commensurate transmitter power and also maintain satisfactory image acuity.

It is reasonable to expect that in the future, application of integrated circuits would further enhance this system. Each channel's amplifier and signal storage network might be deposited directly onto the image array.

BIBLIOGRAPHY

1 Jenkins, F.A., and H.E. White. Fundamentals of Optics, McGraw-Hill, New York, 1950.

2 Kinsler, L.E., and A.R. Frey, Fundamentals of Acoustics, John Wiley & Sons, Inc., New York, 1962.

3 Mellen, R.H., "The Thermal-Noise Limit in the Detection of Underwater Acoustic Signals", The Journal of the Acoustical Society of America, v.24, no.5, Sept. 1952, 478-480.

4 Haslett, R.W.G. et al. "The Underwater Acoustic Camera," Acustica, v.17, no.4, 1966, 187-302.

5 Silver, S., Microwave Antenna Theory and Design, McGraw-Hill, New York, 1949, 169-199.

6 The Microwave Engineer's Handbook and Buyers' Guide 1967, 118-168

7 Folds, D.L., et al. "The Focusing Properties of Liquid Filled Cylindrical Acoustic Lenses With $d/\lambda > 15$", U.S. Navy Mine Defense Lab, Panama City, Fla. Text of presentation at Nov. 1966 meeting of the Acoustical Society of America.

8 Smyth, C.N., et al. "The Ultra-Sound Image Camera", Proceedings I.E.E. (London), v.110, no.1, Jan. 1963, 16-28

9 Hansen, R.C. Microwave Scanning Antennas, Academic Press, New York, 1964-1966, v.1, 74-79.

10 Barta, A.F. "A Time Multiplex Switching System for Visual Display of the Outputs of an Ultrasonic Transducer Array", Thesis, Naval Postgraduate School, Monterey, 1967.

INITIAL DISTRIBUTION LIST

		No. Copies
1.	Defense Documentation Center Cameron Station Alexandria, Virginia 22314	20
2.	Library Naval Postgraduate School Monterey, California 93940	2
3.	Mr. R. G. Wickenden Code 4047, NOTS China Lake, California	1
4.	Prof. G. L. Sackman Department of Electrical Engineering Naval Postgraduate School Monterey, California 93940	3
5.	LT. Kenneth G. Robinson, USN Commander Fleet Air Wing One FPO San Francisco 96670	1

DOCUMENT CONTROL DATA - R&D

(Security classification of title, body of abstract and indexing annotation must be entered when the overall report is classified)

1. ORIGINATING ACTIVITY *(Corporate author)*
Naval Postgraduate School
Monterey, California, 93940

2a. REPORT SECURITY CLASSIFICATION
Unclassified

2b. GROUP

3. REPORT TITLE
An Experimental Ultrasonic Image System For Underwater Vision

4. DESCRIPTIVE NOTES *(Type of report and inclusive dates)*
Thesis (Master of Science)

5. AUTHOR(S) *(Last name, first name, initial)*
ROBINSON, Kenneth G., LT. USN

6. REPORT DATE	7a. TOTAL NO. OF PAGES	7b. NO. OF REFS
June 1967	45	10

8a. CONTRACT OR GRANT NO.

b. PROJECT NO.

c.

d.

9a. ORIGINATOR'S REPORT NUMBER(S)

9b. OTHER REPORT NO(S) *(Any other numbers that may be assigned this report)*

10. AVAILABILITY/LIMITATION NOTICES
[redacted]

11. SUPPLEMENTARY NOTES

12. SPONSORING MILITARY ACTIVITY
Naval Postgraduate School
Monterey, California, 93940

13. ABSTRACT

An experimental investigation of acoustic imaging in water is made at an ultrasonic frequency of 455 KHz. Using optical principles, the theory of image formation and resolution are discussed. The range capability of such a system is predicted by the use of underwater acoustic theory.

The apparatus consists of a basic imaging system that provides a set of d.c. voltages, proportional to sound intensity at points in the image plane, to be applied to a visual display system. Such a display will present a two dimensional image of an insonified underwater target.

This study differs from previous work done in underwater acoustic imaging, in that the image conversion process will lend itself to the application of integrated circuits.

14 KEY WORDS	LINK A		LINK B		LINK C	
	ROLE	WT	ROLE	WT	ROLE	WT
Ultrasonic						
Acoustic Imaging						
Converter						
Imaging						
Image Array						
Underwater Acoustics						